Rapid Coal Devolatilization As an Equilibrium Flash Distillation

A model for the rapid devolatilization of individual coal particles is developed by analogy with a single-stage equilibrium flash distillation. In the theory, thermal depolymerization of the coal generates aromatic fragments that are widely distributed in size. Conditions for phase equilibrium determine the partitioning of these fragments into intermediates in the condensed phase, which ultimately form char and light gas, and into tar vapor, which escapes in a stream of light gases. Comparison with data shows that the model accurately correlates the yields of noncondensible gas and tar from bituminous coals over wide ranges of temperature and pressure. The predicted molecular weight distributions of tar are also in agreement with measured distributions, and the model yields a mechanistic basis for their observed insensitivity to temperature. The tendency to form lighter tar at higher pressures is also explained.

Stephen Niksa
High Temperature Gasdynamics Laboratory
Mechanical Engineering Department
Stanford University
Stanford, CA 94305

Introduction

In devolatilization, coal particles are heated to convert most of the organic coal mass, hydrogen, oxygen, nitrogen, and sulfur into gases. Volatiles consist of permanent gases with high heating value, light oils suitable as fuels, and high-boiling tars for subsequent refining. Tar is a mixture of aromatic compounds of molecular weights from 100 to more than 1,000 whose chemical structure closely resembles that of the parent coal. Char, the porous solid residue, consists of extensive, condensed-ring aromatic structures.

The impact of devolatilization on energy utilization, ignition and flame stability, product quality, and pollutant abatement has prompted an extensive characterization of the important processing conditions. Elevating the temperature or reducing the ambient pressure increases the ultimate yields of volatiles (Anthony et al., 1975). For high-volatile bituminous coals, tar yields from vacuum pyrolysis can be 50% greater than from high-pressure pyrolysis. Yields are enhanced by faster heating at moderate temperatures, but only under vacuum (Niksa et al., 1985). Similarly, yields are enhanced by reducing particle size under vacuum (Niksa et al., 1982; Heyd, 1982), but not at atmospheric pressure (Anthony et al., 1975; Suuberg, 1985; Bautista et al., 1986). Ultimate volatiles yields are remarkably constant (at about 50 wt. %) for lignites, subbituminous, and high-volatile bituminous coals, then diminish for coals of higher rank. But the proportions of gases and tar vary widely with coal rank; tar yields are greatest for high volatile bituminous coals, reaching 40 wt. % under reduced pressures (Freihaut et al., 1982).

A rationale for the behavior of different coal types is unavailable, but the dominant processing influences have been explained. A distribution of decomposition energies is the best basis for the temperature dependence of ultimate yields (Howard, 1981). Yield enhancement by faster heating implies competitive chemistry, although important aspects of nonisothermal devolatilization are exhibited by even the single first-order reaction evaluated over a linear temperature ramp (Juntgen and van Heek, 1968; Niksa et al., 1985).

The pressure dependence has long been attributed to redeposition of tar from the gas phase on the time scale for transport of volatiles through the particle surface; see Howard (1981) and Suuberg (1985) for reviews. This scheme correlates reduced yields for elevated pressures, but is inconsistent with several other aspects. First, the time scale for volatiles escape evident in time-resolved weight loss measurements is three orders of magnitude shorter than the observed weight loss transient. Based on measured rates of tar cracking on this time scale, the extent of tar redeposition is inconsequential throughout all pressures of practical interest (Niksa, 1986). In addition, the measured rate of weight loss is the same for pressures between vacuum and 3.45 MPa (Niksa et al., 1982; Heyd, 1982), suggesting again that the primary thermal reactions, not transport, determine the rates of product evolution.

Moreover, mass transfer limitations are usually apparent in yield or rate measurements for a range of particle sizes, provided that all other conditions can be held constant. For pyrolysis in entrained flow systems, the heat transfer and, consequently, the fuel's thermal history are altered as the particle size is varied, and evidence of any independent influences of mass transfer is obscured (Howard, 1981). But this complication has been eliminated in several wire-grid experiments in which the coal sample was small enough to be dispersed in a layer only a few particles deep. Five such studies have been reported for a range of sizes for the pyrolysis of five coals at similar heating rates (ca. 1,000 K/s), temperatures (1,200–1,300 K), and pressures (0.1 MPa) for reaction times sufficient to achieve ultimate yields. These data appear in Figure 1 and Table 1. In the results of Anthony et al. (1975), the weight loss decreases by 3 wt. % for sizes from 70 to 1,000 μm. This is the largest size effect reported for atmospheric pyrolysis although, since the extent of this apparent size effect is only one-half of the variation in the weight loss from 70 μm particles at 1,250 K in Anthony's temperature study (Figure 12.8; cf. Figure 12.9 in Howard, 1981), it may not be statistically significant. The results of Suuberg (1977) appear in Figure 1 with the least-squares linear regression line. The weight loss correlation decreases by only 1.6 wt. % for sizes from 70 to 920 μm, which is also within the experimental uncertainty. The corresponding tar yields, which appear in Table 1, also show no systematic variation with particle size. In Bautista's (1984) study of size effects, three coals were examined, including a low-volatile sample that does not soften or swell. As seen in Table 1, neither the total weight loss nor the tar yields from any of these coals varied for particle sizes between 80 and 180 μm.

The absence of size effects, the uniform rates of devolatilization at all pressures, and the scaling for negligible homogeneous tar deposition for all pressures of interest are inconsistent with the transport/redeposition scheme. Nor does the size effect in vacuum pyrolysis support this scheme, because all analyses indicate that redeposition becomes negligible in vacuum (Suuberg, 1985). Hence, it seems more likely that char forms from intermediates in the condensed phase, not from tar vapor. The char

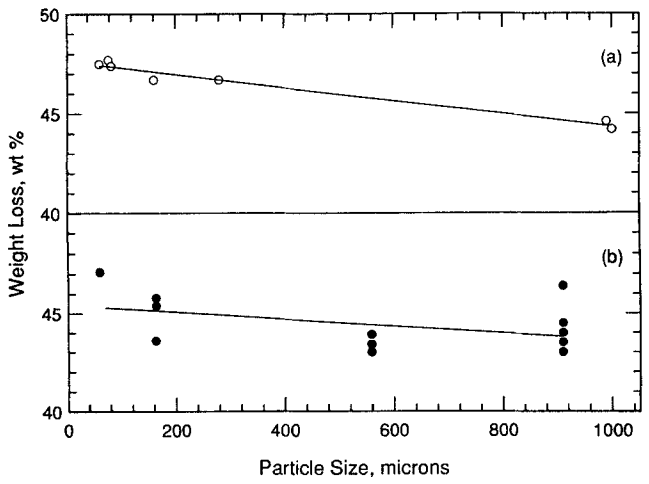

Figure 1. Particle size effects on ultimate weight loss from an HVA bituminous coal, atmospheric pyrolysis.
(a) Anthony et al. (1975)
(b) Suuberg (1977)

Table 1. Ultimate Tar Yields and Weight Loss from Atmospheric Pyrolysis for Various Particle Sizes

Particle Size* μm	Tar Yield* wt. %
149–177	21.8
<300	24.2
297–833	21.2
297–833	21.3
833–991	16.7

Particle Size* μm	Weight Loss/Tar Yields from Three Coals**		
	HVA	LVB	HVA
81	40.4/27.9	—	40.7/30.4
127	41.1/29.5	19.6/14.5	39.3/32.4
180	40.3/30.8	19.3/18.1	40.4/31.1

*Data of Suuberg (1977)
**Data of Bautista (1984)

formation rate in the condensed phase must be orders of magnitude faster than in the vapor, because the concentration of char precursors is that much greater in the condensed phase.

Finally, no quantitative theory has shown why the molecular weight distributions (MWD) of tar shift toward lower molecular weights as the ambient pressure is increased, or why the MWD's are insensitive to temperature (Unger and Suuberg, 1984; Suuberg et al., 1985).

An alternative explanation for the influence of pressure circumvents these inconsistencies, and also accounts for the behavior of tar MWD's. Its central feature is a phase equilibrium among intermediates in the condensed phase and tar components in the vapor phase. At high pressure, the phase equilibrium retains lighter species in the condensed intermediate, which condense into char, thereby reducing the yield of volatiles. James and Mills (1976) introduced this scheme and established its correct qualitative performance. Niksa's (1982) rendition, also qualitative, invoked a scaling in which the internal and ambient pressures are equivalent (except in vacuum), gas-phase redeposition is absent, and all product evolution rates are established by chemical kinetics. Suuberg's models are somewhat different, being analogous to droplet evaporation (Suuberg et al., 1978; Unger and Suuberg, 1981). They envision an equilibrium tar concentration over the external surface of the particle, and a tar evolution rate limited by film diffusion into the ambience.

The reaction model introduced here describes the phase equilibrium in terms of the molecular weight distributions of condensed-phase intermediates and tar components, to explain the observed shifts in tar MWD for ranges of pressure and temperature. It interprets coal devolatilization as a single-stage equilibrium flash distillation driven by two chemical reactions. The mathematical formulation accommodates transport, but transport resistances are deemed negligible for the particle sizes considered in the comparisons with data, and gas-phase tar deposition is omitted. The product evolution rates are established by the chemical reaction rates and therefore are independent of pressure and particle size. Nevertheless, the phase equilibrium shifts to retain intermediates in the condensed phase at elevated pressures, thereby reducing the tar yields.

The empirical basis for each element is discussed in the next section, followed by a derivation of the model and the scaling for

negligible transport resistances. Then the model predictions are evaluated against measured transient and ultimate yields of gas and tar and tar MWD's from bituminous coals for wide ranges of temperature and pressure.

Elements of the Model

This theory develops an analogy between coal devolatilization and a single-stage equilibrium flash distillation. There are only three elements in the model:

1. Primary thermal reactions generate fragments of the coal macromolecule, including those small enough to evaporate and escape as tar
2. The partitioning of these depolymerization fragments into intermediates in the condensed phase (metaplast) and tar vapor follows a phase equilibium represented as Raoult's law for continuous mixtures
3. Metaplast condenses into char, simultaneously forming noncondensible gases

These reaction mechanisms are analyzed in terms of gross species lumps rather than functional groups to avoid the laboratory prerequisites and to minimize the number of adjustable parameters. Coal is represented as reactant units of a molecular weight sufficient to spawn the molecular components of both metaplast and tar; the unit molecular weight is on the order of several thousand. Bridge dissociations within the coal units U generate a mixture of primary fragments of the same chemical constitution, but of lower molecular weight. Among the functional groups in coal, bridges are distinguished from peripheral groups by their enormous range of dissociation energies (Gavalas et al., 1981; Niksa and Kerstein, 1986). Although the actual distribution of energies cannot be measured, a continuous distribution function adequately depicts their very broad thermal response. Despite contrary observations in model compound studies (Allen and Gavalas, 1984), the rate of bridge scission is based on the same frequency factor to avoid unnecessary parameters.

The primary decomposition fragments D are analogous to the throughput of a multicomponent feed stream. They partition into metaplast M, a relatively heavy mixture that remains in the condensed phase, and tar H, the portion of the primary fragments that is light enough to evaporate. The collection of sizes within these three reaction species is represented by continuous functions of molecular weight, as specified below. The chemical constitution of coal units, primary fragments, metaplast compounds, and tar compounds is taken to be the same. This is plausible insofar as the elemental composition and the functional group content of tar and its parent coal are virtually identical for bituminous coals (Solomon and Colket, 1979). However, the model species are not coal constituents; due to their large size, the model species comprise many actual coal nuclei, bridges, and peripheral groups.

As depicted in Figure 2, the porous fuel particle is analogous to the flash chamber. The vapor consists of a binary mixture of tar and light gas that, in softening coals, is dispersed throughout the melt as small bubbles in a viscous liquid; otherwise it is dispersed in a pore system that delineates solid subunits a few hundred Angstroms in size (the size of mesopores). Regardless of the state of the condensed phase, the composition of solid matter is taken to be uniform at any instant. Under the restriction of negligible internal heat transfer resistances, the particle is isothermal.

But the internal pressure must accommodate the generation rate of gases and the resistance to escape. The internal pressure is ambiguous because coal's physical structure admits several plausible transport mechanisms and the transport coefficients are uncertain. Nevertheless, since there is no size effect for atmospheric pyrolysis, the pressure difference for escape by bulk flow must be significantly less than one atmosphere, and it seems likely that the internal and ambient pressures are nearly equivalent (except in vacuum pyrolysis). To maintain a fixed internal pressure, the light gases escape at their rate of production by chemical reaction. Tar evolution is also specified by this

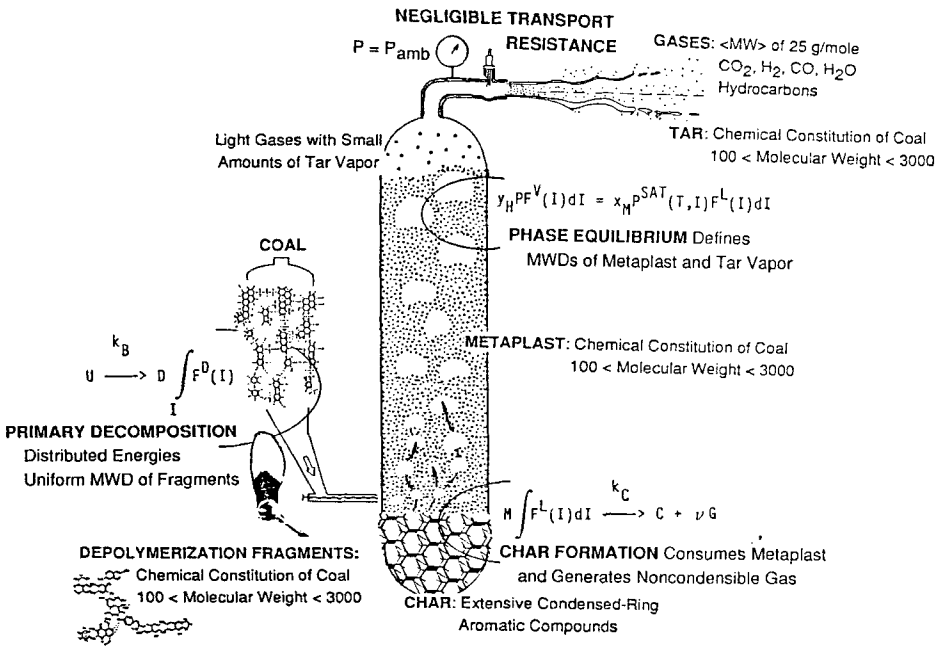

Figure 2. Analogy between a single-stage equilibrium flash distillation and coal devolatilization.

rate, with the additional constraint that phase equilibrium is maintained while the tar vapor is within the particle.

The concentrations of metaplast and tar are related by a generalization of Raoult's law for continuous mixtures that was recently developed for flash calculations (Ratzsch and Kehlen, 1983; Cotterman et al., 1985; Cotterman and Prausnitz, 1985):

$$y_H P F^V(I)dI = x_M P^{sat}(T, I) F^L(I)dI \tag{1}$$

where y_H = mole fraction of tar vapor, based on the concentrations of tar and light gases, P = pressure within the particle, F^V = tar MWD, x_M = mole fraction of metaplast, based on the concentrations of metaplast, coal units, and char, P^{sat} = saturated vapor pressure of metaplast, as a function of temperature T and molecular weight I, F^L = metaplast MWD. This simple form is in keeping with the lack of data on the volatility of coal tar, and is justified by very small mole fractions of both continuous mixtures in their respective phases. Although the saturated vapor pressure of metaplast cannot be measured, that of aromatic coal liquids is of the form

$$P^{sat}(T, I) = P_c \exp(-AI/T) \tag{2}$$

where P_c and A are constants. Unfortunately, the available measurements represent compounds of molecular weight to only 315 (Gray et al., 1985), and cannot be applied directly to the substantially heavier metaplast formed in rapid pyrolysis. In other studies (Suuberg, 1985), $P^{sat}(T, I)$ has been represented with power law functions of molecular weight in the exponent. However, for the sake of mathematical tractability, Eq. 2 is implemented in this model, and P_c and A are regarded as adjustable constants.

Of course, no condensed-phase species leave the particle. But their efflux is analogous to the rate at which metaplast forms char. Char and light gas form when the aromatic nuclei within the metaplast compounds coalesce into refractory compounds, thereby expelling bridges and peripheral groups as light gas:

$$M \int_I F^L(I)\, dI \xrightarrow{k_C} C + \nu G \tag{3}$$

where k_C is a rate constant of Arrhenius form and ν is a stoichiometric coefficient. The proposed elimination of metaplast is independent of its molecular weight, and this unimolecular global step overlooks the repolymerization of metaplast into compounds that may still be volatile.

The connection between char and gas formation is motivated by recent transient measurements of gas yields from a high-volatile bituminous coal. In Figure 3 the yields of various light hydrocarbons and the oxides of carbon measured by Bautista et al. (1986) have been normalized by their ultimate values, and plotted vs. temperature. These results are for uniform heating of a wire grid at 1,000 K/s to the stated temperatures, immediately followed by rapid quenching (at about 5,000 K/s). There was no isothermal reaction period.

Observe that all of these species are generated on similar kinetic time scales except for carbon dioxide, which is evolved much faster than the others. The process underlying this correlation is taken to be char formation, presuming that as nuclei coalesce, peripheral groups and bridges are added, abstracted, and ultimately eliminated by free radical mechanisms. Since the ultimate yields of carbon dioxide from bituminous and high-rank coals are very low (only 1 wt. % in Bautista's study), and the data correlations are currently restricted to such coals, a separate reaction for CO_2 is not included (but will need to be added when low-rank coals are considered).

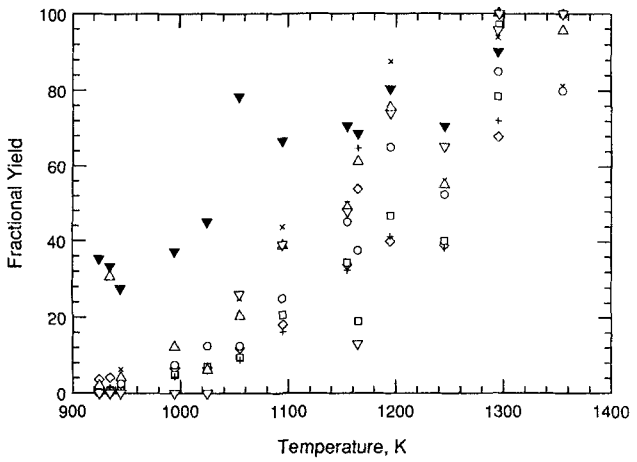

Figure 3. Hydrocarbon yields from an HVA bituminous coal normalized by their ultimate values.

Yields at atmospheric pressure during heat-up at 10^3 K/s with rapid quenching, measured by gas chromatography (Bautista et al., 1986)

▼ CO_2; □ CH_4; ◇ CO; × C_2H_4
+ C_2H_6; △ C_3H_6; ○ C_3H_8; ▽ C_4's

The stoichiometric coefficient for gas production, ν, is related by mass conservation to ratios of molecular weights, according to

$$\nu = \frac{1 - MW_C/MW_U}{MW_G/MW_U} \tag{4}$$

where MW_i is the molecular weight of species i. The numerator is the mass fraction of gas precursors per coal unit, and could be estimated from the relative amounts of aromatic and aliphatic carbon or hydrogen. The molecular weight of gases can be estimated from measured product distributions, and is typically 20–25 g/mol. For a unit molecular weight of 3,000 and a mass fraction of bridges plus peripheral groups of 0.2, ν is 25. The value of ν will diminish with increasing coal rank.

The form of the MWD's for all continuous species can be anticipated. The molar probability densities $F^J(I)$ must vanish below some molecular weight, which delineates noncondensibles from condensibles, increase through a maximum density, then fall off toward the molecular weight of the coal units. Among the distribution functions of this form, it is an empirical fact that the MWD's of coal tar and solvent extracts are very well correlated by the Γ distribution function, which is

$$F(I) = \frac{(I-\gamma)^{\alpha-1}}{\Gamma(\alpha)\beta^{\alpha}} \exp\left[-\frac{(I-\gamma)}{\beta}\right] \tag{5}$$

where $\gamma < I < \infty$, Γ is the gamma function, γ is a shift parameter indicating the origin of $F(I)$, and α, β are adjustable parameters. The mean is $\alpha\beta + \gamma$ and the variance is given by $\alpha\beta^2$. These distributions are normalized to unity over the pertinent range of I.

In Figure 4, measured MWD's of atmospheric and vacuum

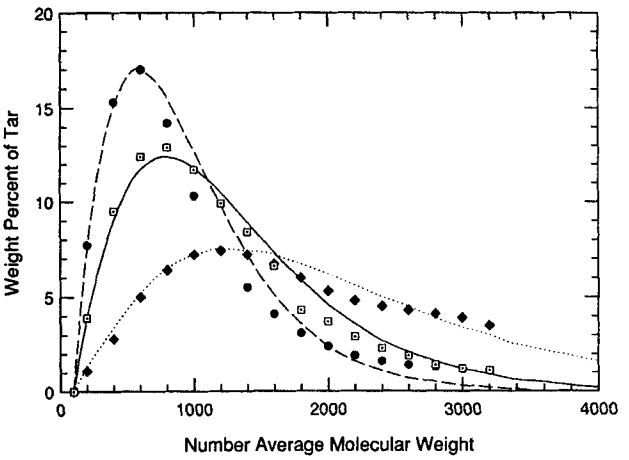

Figure 4. Correlations of MWD's from pyrolysis liquids with the weight-based partially integrated distributions defined in Eq. 6.

Preparation from HVA bituminous coal at a nominal heating rate of 10^3 K/s to 820 K (Unger and Suuberg, 1984):

	β	γ	α
● Atmospheric tar	367	100	1.5
⊡ Vacuum tar	500	100	1.5
♦ Coal extract in THF	825	100	1.5

tars from the pyrolysis of a high-volatile bituminous coal, and of the associated extracts in THF (tetrahydrofuran) (Unger and Suuberg, 1984) are shown with correlations based on Γ distributions. In contrast to the molar probabilities, these MWD's are normalized to unit mass fraction, and partially integrated. Their values indicate the fraction of the total species weight within ±100 units of the value of molecular weight on the abscissa. The relation between the molar probability density $F^J(I)$ and the weight-based MWD, $G^J(I)$, is

$$G^J(I) = \frac{IF^J(I)dI}{\mu_J} \tag{6}$$

The satisfactory correlations of tar and extract MWD's were obtained by varying only the value of β; for the three distributions in Figure 4, the shift parameter is the same and the value of α is also fixed. This latter observation motivates a substantial simplification in the analysis to predict the tar MWD, and we will return to it.

It is reasonable to assume that the MWD of the primary fragments is also a Γ distribution. But quantitatively assigning $F^D(I)$ is ambiguous. Clearly the mean value of F^D is bounded by those of F^V and F^L, but is $F^L(I)$ evident in Fig. 4? Identifying the MWD of coal extracts as $F^L(I)$ is dubious for two reasons. First, solvent extracts have not been related to the precursors to pyrolysis products in any definitive way, and probably include components that are too heavy to affect the equilibrium between tar and metaplast. Second, the technique used to collect the measurements in Figure 4 could not have isolated the intermediates in the partially reacted chars; substantial associations must have occurred while the chars were brought to room temperature. We ignore the MWD's of extracts, and instead regard the measured MWD of vacuum tar as the first approximation to F^D because the fraction of the primary fragments that evaporate is greatest under vacuum.

In this model the MWD of the primary fragments remains the same throughout the disintegration of the coal reactants; i.e., $F^D(I)$ is independent of the extent of pyrolysis. This simplification substantially reduces the model's computational burden, but omits a fundamental aspect of an actual coal depolymerization. Coal devolatilization is an especially complex polymer degradation, in which nuclei liberated by bridge dissociation reattach onto network fragments, thereby forming refractory char links. Such irreversible reattachment diminishes the likelihood of liberating additional small, aromatic nuclei (Niksa and Kerstein, 1986, 1987). Consequently, there is no predetermined concentration of tar precursors, per se, present initially in the coal. Yet this is implied by the coal disintegration step in this model, because all coal units eventually become primary fragments and the lightest of these become tar. In actuality, during devolatilization aromatic nuclei undergo liberation and reattachment concurrently, so many nuclei are never liberated as small fragments and therefore are not subject to the tar formation process.

Overcoming this deficiency involves the methodology developed in our earlier treatments of monomer evolution only (Niksa and Kerstein, 1986, 1987), supplemented with population statistics that describe the complete distribution of fragment sizes. These extensions will identify the evolution of $F^D(I)$ with simultaneous disintegration and integration of a crosslinked macromolecule, and are in progress. Here we avoid a prohibitive computational burden by representing the primary fragments with a uniform distribution function.

Finally, the escape rates of the vapor products are presumed to be proportional to the bulk pressure difference and the mole fractions of the vapor species:

$$J_i = k_m y_i (P - P_O) \tag{7}$$

where J_i = molar escape rate of species i, k_m = a lumped transport coefficient, y_i = mole fraction of vapor species i, P_O = ambient pressure. In this model, the product evolution rates are independent of the transport coefficient, and this crude representation of bulk flow only appears in the scaling for equivalent ambient and internal pressures, and the conditions for negligible resistance to transport.

It is worth repeating that bulk flow is the only escape mechanism compatible with observed volatiles evolution rates; all forms of diffusion are too slow (Russel et al., 1979). Two factors ensure that bulk flow, either through the pore system in nonsoftening coals or through a foaming viscous melt in softening coals, is the actual escape mechanism. First, the change of phase increases the molar volume of any species by three or four orders of magnitude (at atmospheric pressure). Second, the stoichiometry of the thermal reactions further increases the molar volume of vapor species; for light gas evolution, the mole change supplements the molar flux by at least an additional order of magnitude. Consequently, the volatiles escape rate is largely determined by the molar production rate of light gases, while tar is present in minor concentrations and is simply entrained away.

Model Formulation

Reaction species and yields

The model is formulated in terms of scaled molar concentrations (mol/cm^3 original solid) that appear in Table 2. The moles of coal units, primary fragments, metaplast, and char are scaled on the initial concentration of coal units U_O. The molar yield of

Table 2. Reaction Species*

C	Moles of char
D	Moles of primary depolymerization fragments, a continuous mixture
G	Molar concentration of noncondensible gases within the particle
H	Molar concentration of tar within the particle, a continuous mixture
M	Moles of metaplast, a continuous mixture
U	Moles of aromatic coal reaction units
Y_G	Molar yield of noncondensible gases
Y_T	Molar yield of tar

*Concentrations of these species are based on unit coal volume, and are made nondimensional by νU_O for the light gas yield, by C_{VAP} for H and G; and by U_O for all others

tar, Y_T, is also scaled on U_O, while that of light gas, Y_G, is scaled on the product νU_O. The scale factors for the concentrations of tar and gas within the particle are established by the pressure, temperature, and void volume through the ideal gas law. Both G and H are scaled on the total molar concentration in the vapor, which is approximately

$$C_{vap} = \epsilon P_O / RT \tag{8}$$

where ϵ is the void fraction of the condensed phase.

Species mass fractions (wt. % coal) are defined from the molecular weights of reactants and products, since the initial concentration of coal units cannot be measured. The initial bulk density is the product $MW_U U_O$. Since the density is of order unity, the magnitude of U_O is roughly the inverse of MW_U. Species mass fractions W_i are

$$W_i = MW_i U_O S_i / \rho_O = S_i; \quad i = U, D, M, Y_T \tag{9a}$$

where S_i refers to the normalized concentrations designated by i. For light gas,

$$W_G = (1 - MW_C/MW_U) Y_G \tag{9b}$$

and for char

$$W_C = (MW_C/MW_U) C \tag{9c}$$

Note that the initial concentration of coal units, U_O, need not be specified to compute the weight fractions of unreacted coal, char, metaplast, gas, and tar.

Reaction rate equations

It is essential to recognize that the generation rate of primary fragments sets the characteristic time scale for this system. On this basis, the concentrations in the vapor are in quasisteady equilibrium with the changing concentrations of condensed-phase species, and the transport resistance to escape can be neglected. The most rapid time scale is that for maintaining phase equilibrium, followed by the transport time, followed by the time scale for the primary decomposition reactions. Thus, the pertinent nondimensional time is

$$\tau = k_B t = A_B t \exp(-E_O/RT_r) \tag{10}$$

where t is dimensional time; A_B and E_O are parameters in the generation rate of primary fragments; and T_r is the ultimate reaction temperature.

Species conservation is applied in the nondimensional species concentrations defined in the previous section and nondimensional time. Following the derivation of the distributed activation energy model (Anthony et al., 1975), the coal decomposition rate assumes the nondimensional form

$$\frac{dU}{d\tau} = -\int_0^\infty e^{-(E/T - E_O/T)/R} \exp\left[-\int_0^\tau e^{-(E/T - E_O/T_r)/R}\, d\tau'\right] \cdot f(E)\, dE \tag{11}$$

where $f(E)$ is the activation energy distribution; here $f(E) = (1/\sqrt{2\pi}\sigma) \exp[-(E - E_O)^2/\sigma^2]$. Rates of char and light gas formation are based on Eq. 3 and are

$$\frac{dC}{d\tau} = R_C M \int_\gamma^\infty F^L(I)\, dI \tag{12}$$

and

$$\frac{C_{vap}}{U_O}\frac{dG}{d\tau} = R_C M \int_\gamma^\infty F^L(I)\, dI - \frac{dY_G}{d\tau} \tag{13}$$

where $R_C = (A_C/A_B) \exp[-(E_C - E_O)/RT_r]$, a scale for the relative rates of char formation and coal decomposition.

The inventory of the continuous mixtures is formulated for constituents of specific molecular weights, according to

$$\underbrace{\frac{dM}{d\tau} F^L(I)\, dI + \frac{C_{vap}}{U_O}\frac{dH}{d\tau} F^V(I)\, dI}_{\text{Accumulation of liquid and vapor}} = \underbrace{-\left(\frac{dU}{d\tau}\right) F^D(I)\, dI}_{\text{Fragment generation}} \underbrace{- R_C M F^L(I)\, dI}_{\text{Char formation}} \underbrace{- \frac{dY_T}{d\tau} F^V(I)\, dI}_{\text{Tar production}} \tag{14}$$

These four rate equations express molar conservation among the reaction species in equivalent moles of coal units. But only Eqs. 11 and 12 are in final form. We proceed to establish, in turn, the quasisteady equilibration of the vapor concentrations, the equivalent ambient and internal pressures, and the definitions of the MWD's of tar and metaplast in terms of the primary fragment MWD.

A quasisteady equilibrium among the vapor species is evident in the value of the coefficient in the accumulation of light gases in Eq. 13. Specifically, at atmospheric pressure and 1,000 K, for respective values of ϵ, MW_U, and ν of 0.3, 3,000, and 25, $C_{vap}/\nu U_O$ is of the order of 10^{-4}. Consequently, the accumulation of light gas within the particle is entirely negligible, and the gas evolution rate equals the production rate by chemical reaction. Similarly, the accumulation of tar vapor is of the order of 10^{-3}, so that the concentration of tar equilibrates rapidly with the changing concentrations of condensed-phase species. Both accumulation terms for vapor species in the conservation equations should be omitted.

The scaling for equivalent internal and ambient pressures follows from Eq. 13, omitting the accumulation term, and the

transport rate defined by Eq. 7. In nondimensional form,

$$\frac{dY_G}{d\tau} = R_T\delta_p G = R_C M \int_\gamma^\infty F^L(I)\, dI \tag{15}$$

where $R_T = k_M C_{vap} P_O/\nu k_B U_O$, a relative measure of the escape rate and the gas-formation rate, $\delta_p = (P - P_O)/P_O$, a scaled driving force for escape.

Gases and tar are generated on similar time scales, so that the gas evolution rate, $dY_G/d\tau$, must be of order unity. Consequently, balancing the terms in Eq. 15 implies that

$$\delta_p = \delta_O/R_T + O(1/R_T^2) \tag{16a}$$

where δ_O is of order unity. Thus the internal pressure is

$$\frac{P}{P_O} = 1 + O(1/R_T) \tag{16b}$$

Clearly, for short transport times relative to the primary decomposition time ($R_T > 1$), the internal and ambient pressures become equivalent.

But this scaling breaks down if δ_p is not small, as in vacuum pyrolysis. The product evolution rate is still determined by the rate of the primary devolatilization reactions. However, the internal and ambient pressures are certainly not equivalent as P_O goes to zero. The internal pressure reaches a level that is compatible with the transport resistance and the generation rate of volatiles, according to the first equality in Eq. 15. The role of the transport resistance and the fact that the phase equilibrium is especially sensitive to pressure at subatmospheric pressures imply a size dependence in the yields from vacuum pyrolysis, as is observed. Actually, the internal pressure is directly proportional to particle size for escape by continuum flow (represented by Darcy's law) as the ambient pressure goes to zero. This rescaling could be implemented in succeeding relations, but only the case of equivalent internal and ambient pressures is analyzed in what follows.

Whenever the internal and ambient pressures are equivalent, the nondimensional vapor species concentrations, G and H, can be identified as the mole fractions of gas and tar (to order R_T^{-1}). Introducing the species concentrations into the expressions for the fluxes of gas and tar yields the relation between gas and tar evolution:

$$\frac{dY_T}{d\tau} = \frac{\nu H R_T \delta_p}{G} = \frac{\nu H R_C M}{G} \tag{17}$$

Substituting Eq. 17 into Eq. 14 yields the working form of the rate equation for the continuous mixtures:

$$\frac{dM}{d\tau} F^L(I)\, dI = -\left(\frac{dU}{d\tau}\right) F^D(I)\, dI - R_C M F^L(I)\, dI - \frac{\nu H R_C M}{G} F^V(I)\, dI \tag{18}$$

Integrating Eq. 18 with respect to I appears, at first glance, to eliminate all of the MWD's and to close the total mole balance among the reaction species. But the ratio of vapor mole fractions, H/G, is an implicit function of the MWD's. This function must be developed from the relations for phase equilibrium. The stipulation that the mole fractions of the two vapor species sum to unity implies that

$$\frac{H}{G} = \frac{H}{1 - H} \tag{19}$$

The mole fraction of tar vapor, H, is implicitly defined in Raoult's law, Eq. 1, which becomes after introducing the expression for $P^{sat}(T, I)$ and some rearrangement:

$$F^V(I)dI = \left(\frac{x_M P_C}{H P_O}\right) \exp(-AI/T) F^L(I) dI \tag{20}$$

Integrating this expression over the domain of I yields an explicit definition of H, which is

$$H = \frac{\frac{x_M P_c}{P_O} \exp(-\gamma A/T)}{(1 + A\beta_L/T)^{\alpha_L}} \tag{21}$$

and combining Eqs. 19 and 21 yields the desired definition of H/G:

$$\frac{H}{G} = \frac{x_M P_c/P_O}{[\exp(\gamma A/T)(1 + A\beta_L/t)^{\alpha_L} - x_M P_c/P_O]} \tag{22}$$

Observe in Eq. 22 that the relative amount of tar vapor depends on the parameters γ, α_L, and β_L, which define the MWD of metaplast. These parameters as well as those in the MWD of tar are related to those in the MWD of primary fragments below. The relative amount of tar vapor also depends on the ratio of P_c to P_O. This is the explicit form of the mechanism by which the phase equilibrium shifts the partitioning of the primary fragments into the metaplast as the ambient pressure increases. Observe also that because of the subtraction in the denominator, the analysis is restricted to a minimum ambient pressure that is determined by the values of the parameters in Eq. 22. This theory does not apply to vacuum pyrolysis, although the same rate equations could be rescaled to allow the transport resistance to determine the internal pressure whenever $(P - P_O)/P_O$ is not small, as sketched out above.

We settle for an approximate closure of the mole balance over the constituents in the MWD's, by matching moments of Eq. 18. However, before we proceed to close the mole balances, observe that the moments of the metaplast and tar vapor MWD's are not independent. The mean and variance of the metaplast MWD are based on the following moments of a gamma distribution:

$$\mu_L = \int_\gamma^\infty (I - \gamma) F^L(I)\, dI = \alpha_L\beta_L + \gamma \tag{23a}$$

$$\sigma_L^2 = \int_\gamma^\infty (I - \mu_L)^2 F^L(I)\, dI = \alpha_L\beta_L^2 \tag{23b}$$

The moments of the tar MWD need not involve independent distribution parameters, since the tar and metaplast MWD's are related by Eq. 20. The mean and variance of F^V are defined from successive integrations of Eq. 20 after multiplying through by

$(I - \gamma)$ and $(I - \mu_V)^2$, respectively, and they are

$$\mu_V = \frac{\alpha_L \beta_L}{1 + \beta_L A/T} + \gamma \tag{23c}$$

$$\sigma_V^2 = \sigma_L^2 \left(\frac{\mu_V - \gamma}{\mu_L - \gamma}\right)^2 = \frac{\alpha_L \beta_L^2}{(1 + \beta_L A/T)^2} \tag{23d}$$

It is interesting that only the parameter A appears in the relations among the moments of the tar and metaplast MWD's, because the integral of $F^V(I)$ over I is normalized to unity.

The moments of both F^V and F^L appear in the relations that close the mole balance over the constituents in the MWD's. The zero moment is an integration of Eq. 18 over all I, which eliminates all $F^J(I)$ because they are normalized, but still includes distribution parameters through Eq. 22. Its form is apparent from Eq. 18. The first moment obtains from integrating Eq. 18 over I after multiplying through by $I - \gamma$, and yields after rearrangement that involves Eq. 23c:

$$\frac{dM}{d\tau} = -\left(\frac{dU}{d\tau}\right)\frac{\alpha_D \beta_D}{\alpha_L \beta_L} - R_C M + \frac{\nu H R_C M}{G(1 + \beta_L A/T)} \tag{24}$$

The second moment obtains from integrating Eq. 18 over I after multiplying through by $(I - \mu_L)^2$, and yields after rearrangement that involves Eq. 23d:

$$\frac{dM}{d\tau} = -\left(\frac{dU}{d\tau}\right)\left[\frac{\alpha_D \beta_D^2}{\alpha_L \beta_L^2} + \frac{(\alpha_D \beta_D - \alpha_L \beta_L)^2}{\alpha_L \beta_L^2}\right] - R_C M + \frac{\nu H R_C M}{G}\left\{\frac{1 + \alpha_L}{(1 + \beta_L A/T)^2} + \alpha_L\left[1 - \frac{2}{(1 + \beta_L A/T)}\right]\right\} \tag{25}$$

With initial values of unity for U and zero for all other species, and the primary fragment characteristics α_D, β_D, and γ, Eqs. 11–13, 18, and 22–25 constitute a closed set of rate equations for the instantaneous concentrations U, C, M, Y_G, and Y_T, and the MWD characteristics α_L $(=\alpha_V)$, β_L, and β_V. While the instantaneous MWD of metaplast is described by α_L and β_L, the tar MWD must be constructed as a weighted sum of the incremental tar yields and the instantaneous values of α_V and β_V, because the phase equilibrium applies only while the tar vapor is within the particle.

Based on the acceptable correlations in Figure 4 of quite varied MWD's for the same value of α, the second moment equation, Eq. 25, can be eliminated by fixing the values of α for metaplast and tar at those for the primary fragments. Then the zero and first moment equations are combined into an implicit definition of β_L,

$$-\left(\frac{dU}{d\tau}\right)\bar{\beta}(1 - \bar{\beta}) = \frac{(\nu R_c M) x_M \bar{A} P_c}{[P_o e^{\gamma A/T}(1 + \bar{A}/\bar{\beta})^{\alpha} - x_M P_c](1 + \bar{A}/\bar{\beta})} \tag{26}$$

where

$$\bar{\beta} = \beta_D/\beta_L$$

$$\bar{A} = A/\beta_D T$$

The rate equations are solved by coupling a numerical root-finder for Eq. 26 to the program LSODE, a general purpose numerical package for initial value, stiff ordinary differential equations. Simulations of this model require less than 1 min per complete simulation of an AT-type personal computer.

Comparison with Experimental Data

The theory underlying this model is relatively easy to evaluate because there are very few adjustable parameters considering that the model predicts the yields of gas and tar as well as the tar MWD. Values for the model parameters in Table 3 resulted from correlating the measurements in this section. The adjustable parameters are the two reaction rate constants, the stoichiometric coefficient, and the constants in the saturated vapor pressure of metaplast. In contrast to all previous devolatilization models, this model does not include any parameters that set the ultimate yields of any of the products. Instantaneous and ultimate yields of both tar and gas reflect the competition between escape and char formation, which is determined by the thermal history and ambient pressure. Extending the analysis to predict tar MWD's involves no additional parameters, but does add stringency.

The measured product distributions and weight loss in this evaluation were determined with a microsample wire-grid heater, and have been reported separately (Bautista et al., 1986; Niksa et al., 1982). In these experiments the time-temperature histories consist of a linear temperature ramp (constant heating rate), an abrupt turnover to a constant reaction temperature, and immediate quenching after the specified isothermal reaction period. Transient yields were resolved by forced quenching with cold nitrogen, and are regarded as instantaneous values. Ultimate yields refer to the results for reaction periods sufficiently long to achieve asymptotic values as the stated operating conditions. Results are included from two HVA bituminous coal samples that were matched by the Penn State Data Base.

The samples of tar for the MWD measurements were also generated in a screen heater, but in independent studies (Unger and Suuberg, 1984; Suuberg et al., 1985). This heater is not equipped with a quench, so the results are regarded as ultimate values. Only results from the HVA coal are included. The MWD's are based on gel-permeation chromatography using THF as the mobile phase. These MWD's extend to substantially higher molecular weights than those determined in pyridine (Oh, 1985) or with FIMS (field ionization mass spectrometry) (Solomon et al., 1987), which is problematic but not surprising. Notwithstanding these uncertainties, all measured MWD's are consistent in their insensitivity to temperature and in their shift

Table 3. Values of Model Parameters

MWD of Primary Decomposition Fragments
$\gamma = 100$; $\alpha = 1.5$; $\beta_D = 550$

Reaction Rate Parameters

	A-Factor s^{-1}	E_a kJ/mol
Primary decomposition	$3. \times 10^7$	160 ($\sigma = 29.3$)
Char formation	1.5×10^9	146

Molar stoichiometry of light gas per mole char is 22.2
$P^{sat}(T, I) = 7.1 \exp(-1.6\, I/T)$, MPa

to lower molecular weights with increasing pressure, and all are well represented by gamma distributions. The mechanistic bases for these trends are emphasized in what follows. Moreover, by adjusting various parameters the mean values of the predicted tar MWD's can be shifted over a sizable range while the predicted product yields remain the same, as demonstrated in the Appendix.

Figure 5 shows the predicted ultimate distribution of all reaction species and the ultimate weight loss at atmospheric pressure for a heating rate of 10^3 K/s. Coal units are present through 1,200 K as a result of the broad distribution of dissociation energies in the decomposition step, consistent with the substantial volatiles yields for two-step heating (Anthony et al., 1975). Note also that the amount of char increases monotonically with temperature throughout this range. As is evident in the data, the competition between tar and char formation heavily favors char formation during the decomposition of the last half of the coal units, above 900 K. Throughout this temperature range, the correlation of weight loss is within the experimental uncertainty.

The ultimate product distribution of volatiles for the same conditions appears in Figure 6. Here too the correlations are within the experimental uncertainty. At low temperatures, tar is the first product to appear, while gas formation becomes more pronounced at high temperatures. On a mass basis, the proportions of tar and gas range from about 10:1 at 800 K to 3:1 at 1,300 K, reflecting the selectivity to char formation above 900 K. The coupling of gas formation to char formation in this reaction scheme captures this behavior.

Ultimate yields provide a good test for this model, but transient yields during heat-up are more relevant to most coal utilization processes, and more stringent means to evaluate models. The time scale for the primary decomposition reaction, Eq. 10, varies by four orders of magnitude for temperatures from 800 to 1,300 K, and the actual variation is much greater if the activation energy distribution is accounted for. A comparison with transient weight loss and gas yields during heat-up at 10^3 K/s appears in Figure 7. The onset of devolatilization and the yields throughout the linear thermal transient are correlated within the experimental uncertainty, as are the proportions of tar and gas. On a mass basis, tar formation becomes appreciable at

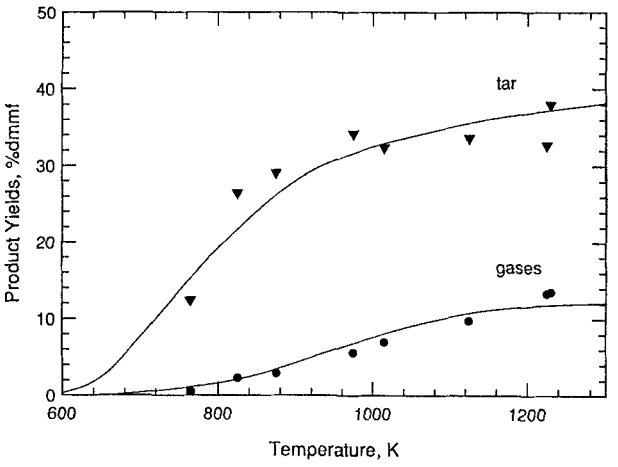

Figure 6. Predictions compared with measured ultimate yields (Bautista et al., 1986).
Pyrolysis as in Figure 5
▼ Tar; ● gases

800 K, 200 K below the onset of gas production. But on a molar basis, light gases are always the major component in the vapor. The computed mole fraction of tar is 0.3 at 800 K, at the onset of devolatilization, but falls quickly and remains at 10^{-2} to 10^{-3} throughout. In all of these simulations, tar is a sparse component that is entrained away in a stream of light gases.

We turn next to the tar MWD's from atmospheric pyrolysis. While no prior devolatilization model has attempted to predict tar MWD's, the comparison in Figure 8 establishes the validity of this aspect of the theory. The data correlation is for tar MWD's on the partially integrated weight basis, defined in Eq. 6, from atmospheric pyrolysis at 820 K. The predictions from the model are as accurate as any curve fit based on the Γ distribution can be, and are probably within the experimental uncertainty throughout. The weight-based MWD of the primary fragments also appears in Figure 8, demonstrating that the model predictions involve a substantial partitioning of the assumed fragment distribution into metaplast and tar. The mean value of the tar MWD is some 275 units less than the mean of the fragment MWD.

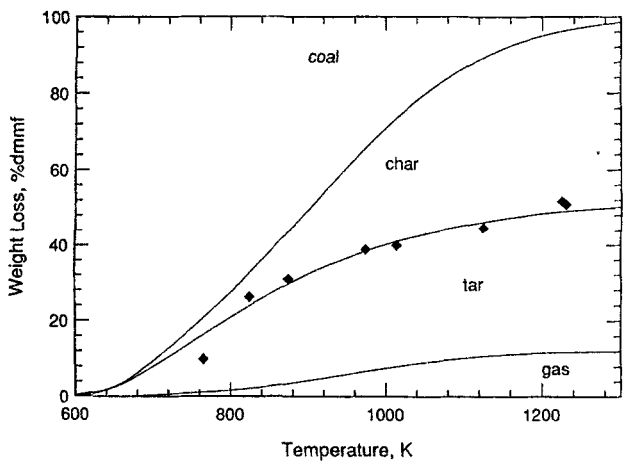

Figure 5. Predicted ultimate distribution of model species compared to measured weight loss (Bautista et al., 1986).
HVA bituminous coal, atmospheric pyrolysis at 10^3 K/s

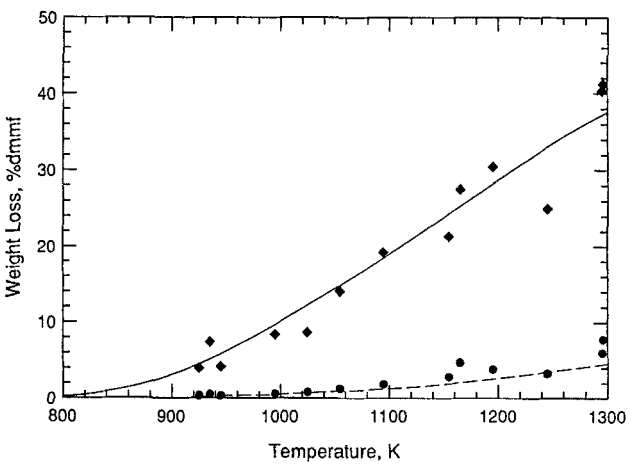

Figure 7. Predictions compared with measured weight loss and gas yields (Bautista et al., 1986).
♦ Weight loss, ● gas yields, during heat-up at 10^3 K/s, atmospheric pressure

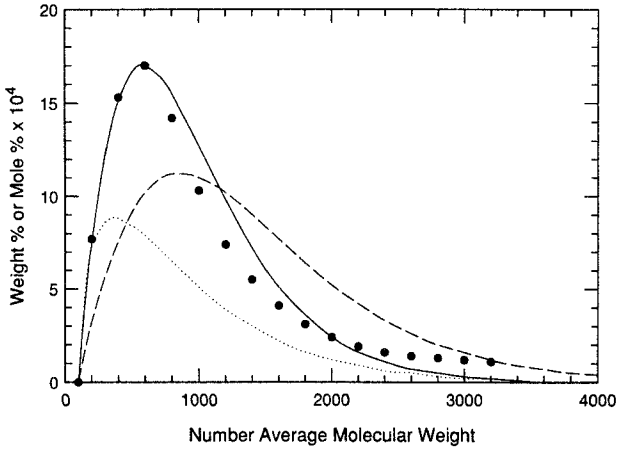

Figure 8. Predicted and measured weight-based tar MWD's from atmospheric pyrolysis at 820 K.

— Predicted; ● measured
--- Molar MWD of primary fragments
··· Weight-based MWD of primary fragments

The fragment MWD on a molar basis is included in Figure 8 to show that a molecular weight of 3,000 for the coal units is a reasonable characteristic value. (The MWD's of coal extracts include substantial amounts of material of molecular weight greater than 3,000.) For $\nu = 22.2$ and $MW_C/MW_U = 0.8$, the predicted average value of the molecular weight of gases is 27, in agreement with Bautista's reported value of 26 for the gases from atmospheric pyrolysis.

Perhaps the most puzzling result from recent laboratory studies is that tar MWD's are insensitive to temperature (Unger and Suuberg, 1984); their mean values increase by only about 100 units for pyrolysis temperatures from 700 to 1,300 K. An earlier, semiquantitative attempt to rationalize such behavior, based on a film-diffusion-limited evaporation scheme, predicted much larger shifts (Suuberg, 1985). But the scheme based on this theory is successful. Figure 9 compares predicted and measured tar MWD's for temperatures between 730 and 1,300 K. The bars through the data points indicate the range of measured values in the MWD's of the various tar samples at each molecular weight. The agreement is remarkably close for the lighter weight components. The minor discrepancies for molecular weights between 800 and 1,600 are due to the imposed form of the distribution functions, not to any defect in the model's underlying mechanisms.

These results seem surprising because the temperature dependence in the saturated vapor pressure of metaplast is indeed strong; the molecular weight dependence in $P^{sat}(T, I)$ ensures that it will be. But two additional mechanisms alter the primary fragment inventory, counteracting the shifting phase equilibrium somewhat. First, coal decomposition extends over a wide range of temperature (due to the broad thermal response of the energy distribution), and replenishes the system with lighter tar precursors throughout this temperature range; as seen in Figure 5, coal units are available through 1,200 K. Second, the accumulation of metaplast supplements the inventory with intermediate-weight compounds. At moderate temperatures such compounds reside in the metaplast, but at higher temperatures they are expelled as tar. Of course this is a factor only during heat-up. But since yields at the end of the heating period to temperatures above 1,150 K are substantial fractions of the ultimate yields, the accumulation of metaplast accounts, in part, for the satisfactory results in Figure 9.

The remaining two elements in this comparison focus on the influence of ambient pressure. The comparison of ultimate weight loss at 1,050 K for a wide range of pressure appears in Figure 10. The correct qualitative trend is evident in the predictions. Volatile yields fall very rapidly as the pressure is increased from vacuum to a few atmospheres, then reach an asymptote. But the model predictions continue to fall, albeit with lower sensitivity, for pressures above 1 MPa. The predicted gas yields increase by 50% as the pressure increases from 0.1 to 3.5 MPa, in accord with an established trend (Suuberg et al., 1978). The quantitative discrepancy is in the tar yields. Although the predicted tar yields are too low at high pressure, they remain substantial throughout this pressure range (W_T at 3.5 MPa is 8 wt. %).

This discrepancy is most likely due to the expedient representation of coal depolymerization in this model. Increasing the pressure substantially increases the metaplast inventory, espe-

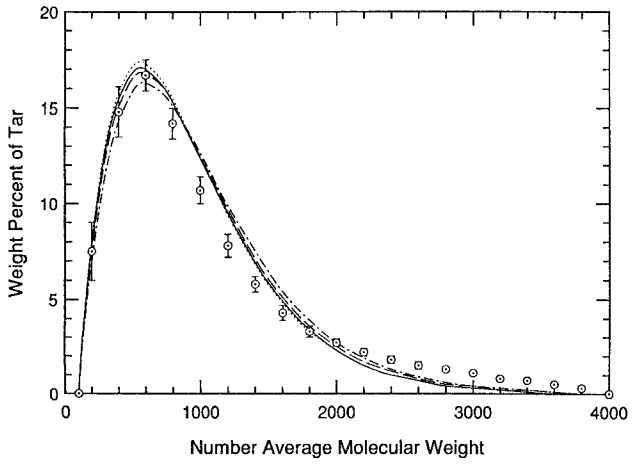

Figure 9. Predicted (curves) and measured weight-based tar MWD's from atmospheric pyrolysis, 703–1,300 K.

⊙ Measured MWD's, I value range observed (Unger and Suuberg, 1984)

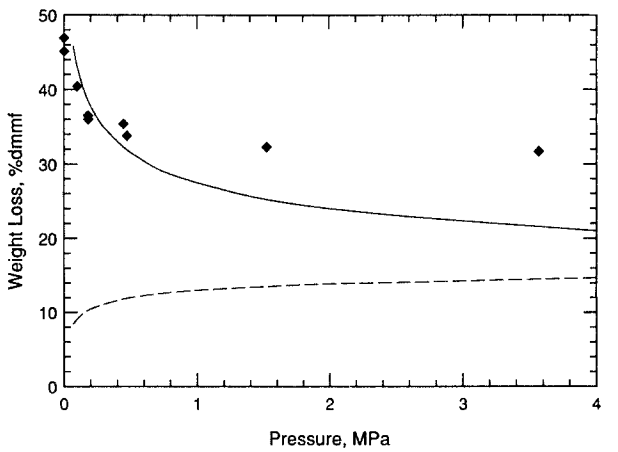

Figure 10. Predicted and measured ultimate weight loss at 1,050 K, 0.07–3.5 MPa.

— Predicted; ♦ measured (Niksa et al., 1982)
--- Predicted yields of light gases

cially of the high molecular weight components of the primary fragments. In this scheme, these components can only be converted into char. But in actuality, metaplast continues to decompose into smaller fragments, replenishing the inventory of species that can vaporize at even the highest ambient pressures. The time scale for metaplast decomposition is the same as that for the primary decomposition (both processes being determined by bridge dissociation), so this explanation is consistent with uniform rates of devolatilization for all pressures.

Even omitting metaplast decomposition, the predicted tar MWD's become substantially enriched in lighter species as the pressure is increased. Weight-based tar MWD's for 0.1, 1, and 3.5 MPa and 1,050 K appear in Figure 11. Increasing pressure does indeed shift the phase equilibrium to suppress tar formation. Observe that compounds of molecular weight below 2,000 are predicted to escape as tar at even the highest pressures of interest. This value is probably too high, because of the omission of metaplast decomposition. While no tar MWD's from high-pressure devolatilization have been measured, the predicted trend lies well within the resolution of current experimental techniques, and needs to be evaluated against data.

Conclusions

Accurate single-particle models of coal devolatilization must account for widely varied operating conditions, especially temperature and pressure. On the other hand, only models that are computationally expedient can pave the way for better full-scale combustor and gasifier simulators. This theory was developed with these conflicting demands in mind and its description of temperature and pressure effects is encouraging.

Data correlations of the yields from high-volatile bituminous coals for temperatures to 1,300 K are within the experimental uncertainty, including the proportions of tar and light gas during heat-up and for reaction periods long enough to achieve ultimate values. For the first time tar MWD's are correlated within the experimental uncertainty, and a quantitative basis for their observed insensitivity to temperature is available. The activation energy distribution, metaplast accumulation, and devolatilization during heat-up are needed to explain why measured tar MWD's are insensitive to temperature.

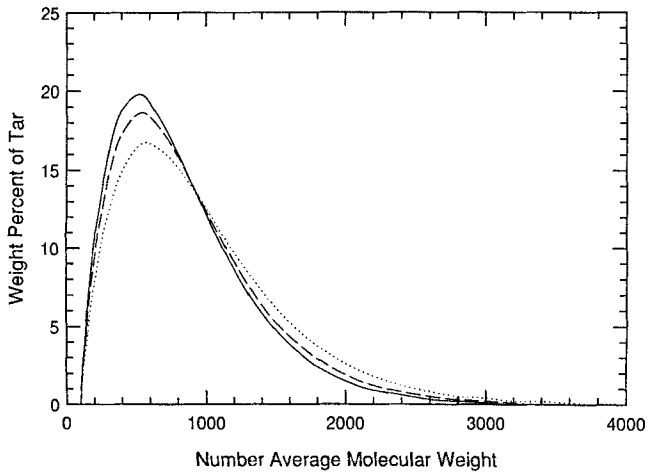

Figure 11. Predicted weight-based tar MWD's for 1,050 K.

··· at 0.1 MPa; --- at 1.0 Mpa; — at 3.5 MPa

The tendency to form lighter tar at higher pressures is also explained. As the pressure is increased, a progressively smaller portion of the heavier fragments has a vapor pressure that is comparable to the ambient pressure, as required for evaporation. Fragments meeting this criterion at low pressure are retained in the metaplast at high pressure, and ultimately are converted into char. And as more char forms, the yields of light gas increase. Thus, the model exhibits the correct behavior of reduced tar yields, lighter tar MWD, and increased gas yields with increasing pressure. Qualitatively, the predicted influence of pressure on product yields is sound, although predicted tar yields at pressures above 1 MPa are too low, due to the expedient treatment of coal depolymerization. The predicted gas yields are reliable throughout the relevant pressure range.

The scaling for negligible transport resistances is consistent with the lack of a particle size effect for atmospheric pyrolysis; it also rationalizes the particle size effect in vacuum (although this model does not apply to vacuum pyrolysis). And basing the product evolution rates on the rates of the primary decomposition reactions ensures equal devolatilization rates for all pressures, in agreement with measurements.

Extensions already underway are addressing the network statistics for the depolymerization step and accounting for the heat and mass transport from the free stream during pulverized coal combustion, to model ignition. Although the theory is developed for coal devolatilization, with only minor modifications it can be adapted to the devolatilization of charring polymers and biomass, and the evaporation and combustion of residual fuel oils.

Acknowledgment

This work was supported by a contract with the Electric Power Research Institute. The author is also grateful to Chun Lau of the Mechanical Engineering Department at Stanford University for bringing the rate equations for the continuous mixtures into final form, and for helping with the simulations.

Notation

$\underline{A}$ = adjustable constant in $P^{sat}(T, I)$
$\bar{A}$ = parameter $A\beta_D/T$
A_B = frequency factor for primary decomposition
C_{vap} = molar concentration of vapor per coal volume
E = dissociation energy for primary decomposition
E_O = mean dissociation energy for primary decomposition
$F^J(I)$ = normalized molar probability density function of J
$f(E)$ = distribution of energies for primary decomposition
$G^J(I)$ = weight-based, partially integrated MWD of J
I = molecular weight in any of the continuous mixtures
J_i = molar transport rate of species i by bulk flow
k_B = characteristic Arrhenius reaction rate constant for primary decomposition, evaluated at A_B and E_O
k_C = Arrhenius rate constant for char formation
k_m = lumped transport coefficient for bulk flow
MW_i = molecular weight of reaction species i
P = pressure within the coal particle
P_O = ambient pressure
P_c = adjustable coefficient in $P^{sat}(T, I)$
$P^{sat}(T, I)$ = saturated vapor pressure of metaplast
R = gas constant
R_C = scale for char formation vs. primary decomposition
R_T = scale for escape by bulk flow vs. gas formation
t = dimensional time
T = instantaneous temperature
T_r = ultimate reaction temperature
U_O = initial moles of coal units per unit coal volume
W_i = species mass fractions in wt. % coal
x_M = mole fraction of metaplast

Y_i = molar yield of vapor species i
y_H = mole fraction of tar vapor

Greek letters

α = adjustable constant in Γ distribution function
β_i = adjustable constant in Γ distribution function of continuous mixture i
$\bar{\beta} = \beta_D/\beta_L$
γ = shift parameter in Γ distribution function
δ_p = scaled pressure difference for bulk flow
ϵ = particle void volume per unit coal volume
μ_i = mean value in MWD's of continuous mixtures
ν = molar stoichiometric coefficient for gas formation
ρ_O = initial bulk coal density
σ = standard deviation of dissociation energy distribution for primary decomposition
σ_i^2 = variance of MWD of continuous mixture i
τ = nondimensional time

Subscripts

C = char
D = primary decomposition fragments
G = light gas
L = size characteristics of metaplast
T = tar
U = coal units
V = size characteristics of tar vapor

Superscripts

D = size characteristics of primary decomposition fragments
L = size characteristics of metaplast
V = size characteristics of tar vapor

Appendix

Notwithstanding the current experimental uncertainties in the mean molecular weight of tar, all measured MWD's are consistent in their insensitivity to temperature and in their shift to lower molecular weights with increasing pressure, and all are also well represented by gamma distributions. The parametric studies in this section demonstrate that the uncertain magnitudes of tar MWD do not undermine the theory's correct depiction of the influences of temperature and pressure on the product yields and tar MWD's.

The behavior of this model is governed by nondimensional groups formed from its adjustable parameters; i.e., those in the two reaction rate constants, the stoichiometric coefficient, the two constants in $P^{sat}(T, I)$, and β_D. (In the primary fragment MWD both γ and α were assigned independently.) The nondimensional groups were identified, in part, from approximate analytical solutions for isothermal pyrolysis. The parametric dependence of the ultimate tar yields, W_T, involves four parameters, according to

$$W_T = W_T(\eta, R_c, \bar{A}, \nu) \tag{A1}$$

where

$$\eta = (\nu - 1)\left[\frac{P_o R_c \exp(-\gamma A/T)}{\nu P_c}\right]^{1/2}$$

and all other parameters are defined in the body of the paper. The mean molecular weight of tar, μ_v, depends on these same four parameters and independently on β_D, according to

$$\mu_v = \mu_v(\eta, R_c, \bar{A}, \nu, \beta_D) \tag{A2}$$

Although the tar yields do depend on β_D (through $\bar{A}$), the sensitivity is weak. But the independent influence of β_D on the mean molecular weight of tar is strong, and this feature allows μ_v to be shifted substantially while the yields of tar remain the same. In Figure A1, ultimate tar yields and mean tar molecular weights predicted for atmospheric pyrolysis at 1,000 K are plotted vs. $\bar{A}$. Only the values of A and β_D were varied in these simulations; values of all other parameters appear in Table 3. The solid and dashed curves represent variations in $\bar{A}$ due respectively to variations in A (case A) and to variations in β_D (case B).

The tar yields for both cases are essentially the same, and in accord with the parametric dependencies in Eq. A1. But the independent influence of β_D on μ_v is striking. Mean molecular weights of tar are very sensitive to $\bar{A}$, but change in opposite directions for these two cases. Consequently, μ_v can be shifted by hundreds of units by varying A and β_D within the constraint of fixed $\bar{A}$, without affecting the correlations of measured tar yields, or the theory's correct depiction of the influences of temperature and pressure variations on tar MWD's.

Literature Cited

Allen. D. T., and Gavalas, G. R., "Reactions of Methylene and Ether Bridges," *Fuel*, **63**, 586 (1984).

Anthony, D. B., J. B. Howard, H. C. Hottel, and H. P. Meissner, "Rapid Devolatilization of Pulverized Coal," *15th Int. Symp. Combustion*, Combust. Inst., Pittsburgh, 1303 (1975).

Bautista, J. R., "Time-Resolved Pyrolysis Product Distributions from Softening Coals," Ph.D. Thesis, Dept. Chem. Eng., Princeton Univ. (1984).

Bautista, J. R., W. B. Russel, and D. A. Saville, "Time-Resolved Pyrolysis Product Distributions of Softening Coals," *Ind. Eng. Chem. Fundam.*, **25**, 536 (1986).

Cotterman, R. L., and J. M. Prausnitz, "Flash Calculations for Continuous or Semicontinuous Mixtures Using an Equation of State," *Ind. Eng. Chem. Process Des. Dev.*, **24**, 434 (1985).

Cotterman, R. L., R. Bender, and J. M. Prausnitz, "Phase Equilibria for Mixtures Containing Very Many Components. Development and Application of Continuous Thermodynamics for Chemical Process Design," *Ind. Eng. Chem. Process Des. Dev.*, **24**, 194 (1985).

Freihaut, J. D., M. F. Zabielski, and D. J. Seery, "A Parametric Investigation of Tar Release in Coal Devolatilization," *19th Int. Symp. Combustion*, Combust. Inst., Pittsburgh, 1159 (1982).

Gavalas, G. R., P. H. Cheong, and R. Jain, "Model of Coal Pyrolysis. 1: Qualitative Development," *Ind. Eng. Chem. Fundam.*, **20**, 113 (1981).

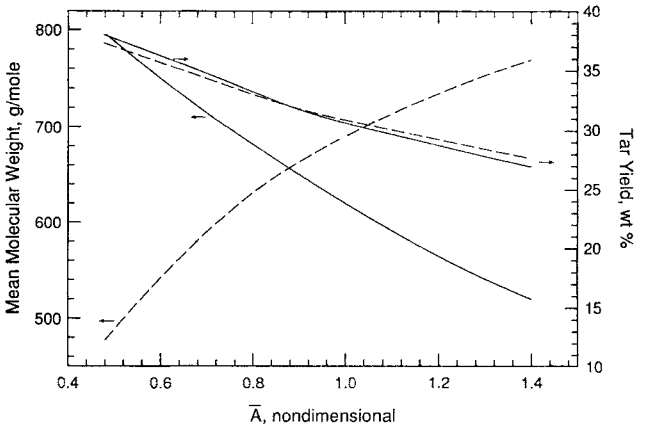

Figure A1. Predicted ultimate yields and mean molecular weights of tar vs. $\bar{A} \equiv A\beta_D/T$.

Atmospheric pyrolysis at 1,000 K; reaction rate parameters as in Table 3
— Case A: variations in $\bar{A}$ for $0.873 < A < 2.545$ at $\beta_D = 550$
--- Case B: variations in $\bar{A}$ for $300 < \beta_D < 875$ at $A = 1.6$

Gray, J. A., G. E. Holder, C. J. Brady, J. R. Cunningham, J. R. Freeman, and G. M. Wilson, "Thermophysical Properties of Coal Liquids. 3: Vapor Pressure and Heat of Vaporization of Narrow-Boiling Coal Liquid Fractions," *Ind. Eng. Chem. Process Des. Dev.*, **24**, 97 (1985).

Heyd, L. E., "Weight Loss Behavior of Coal During Rapid Pyrolysis and Hydropyrolysis," M.S. Thesis, Dept. Chem. Eng., Princeton Univ. (1982).

Howard, J. B., "Fundamentals of Coal Pyrolysis and Hydropyrolysis," *Chemistry of Coal Utilization*, 2nd supp. vol., M. A. Elliot, ed., Wiley-Interscience, New York, ch. 12 (1981).

James, R. K., and A. F. Mills, "Analysis of Coal Particle Pyrolysis," *Lett. Heat Mass Trans.*, **3**, 1 (1976).

Juntgen, H., and K. H. van Heek, "Gas Release from Coal as a Function of the Rate of Heating," *Fuel*, **47**, 103 (1968).

Niksa, S., "Time-Resolved Kinetics of Rapid Coal Devolatilization," Ph.D. Thesis, Dept. Chem. Eng., Princeton Univ. (1982).

———, "The Distributed-Energy Chain Model for Rapid Coal Devolatilization Kinetics. II: Transient Weight Loss Correlations," *Combust. Flame*, **66**, 111 (1986).

Niksa, S., and A. R. Kerstein, "The Distributed-Energy Chain Model for Rapid Coal Devolatilization Kinetics. I: Formulation," *Combust. Flame*, **66**, 95 (1986).

———, "On the Role of Macromolecular Configuration in Rapid Coal Devolatilization," *Fuel*, **66**, 1389 (1987).

Niksa, S., W. B. Russel, and D. A. Saville, "Time-Resolved Weight Loss Kinetics for the Rapid Devolatilization of a Bituminous Coal," *19th Int. Symp. Combustion*, Combust. Inst., Pittsburgh, 1151 (1982).

Niksa, S., L. E. Heyd, W. G. Russel, and D. A. Saville, "On the Role of Heating Rate in Rapid Coal Devolatilization," *20th Int. Symp. Combustion*, Combust. Inst., Pittsburgh, 1445 (1985).

Oh, M. S., "Softening Coal Pyrolysis," Sc.D. Thesis, Dept. Chem. Eng., MIT (1985).

Ratzsch, M. T., and H. Kehlen, "Continuous Thermodynamics of Complex Mixtures," *Fluid Ph. Equil.*, **14**, 225 (1983).

Russel, W. B., D. A. Saville, and M. I. Greene, "A Model for Short Residence Time Hydropyrolysis of Single Coal Particles," *AIChE J.*, **25**, 65 (1979).

Solomon, P. R., and M. B. Colket, "Coal Devolatilization," *17th Int. Symp. Combustion*, Combust. Inst., Pittsburgh, 131 (1979).

Solomon, P. R., D. G. Hamblen, R. M. Carangelo, M. A. Serio, and G. V. Deshpande, "A General Model of Coal Devolatilization," *Am. Chem. Soc. Div. Fuel Chem. Pre.*, **32**(3), 83 (1987).

Suuberg, E. M., "Rapid Pyrolysis and Hydropyrolysis of Coal," Sc.D. Thesis, Dept. Chem. Eng., MIT (1977).

———, "Mass Transfer Effects in Pyrolysis of Coals: A Review of Experimental Evidence and Models," *Chemistry of Coal Conversion*, R. H. Schlosberg, ed., Plenum, New York, ch. 4 (1985).

Suuberg, E. M., W. A. Peters, and J. B. Howard, "Product Compositions and Formation Kinetics in Rapid Pyrolysis of Pulverized Coal—Implications for Combustion," *17th Int. Symp. Combustion*, Combust. Inst., Pittsburgh, 117 (1978).

Suuberg, E. M., P. E. Unger, and W. D. Lilly, "Experimental Study on Mass Transfer from Pyrolysing Coal Particles," *Fuel*, **64**, 966 (1985).

Unger, P. E., and E. M. Suuberg, "Modeling the Devolatilization Behavior of a Softening Bituminous Coal," *18th Int. Symp. Combustion*, Combust. Inst., Pittsburgh, 1203 (1981).

———, "Molecular Weight Distributions of Tars Produced by Flash Pyrolysis of Coals," *Fuel*, **63**, 606 (1984).

Manuscript received Aug. 18, 1987, and revision Dec. 17, 1987.